

Interpretable and Generalizable Person Re-identification with Query-adaptive Convolution and Temporal Lifting

Shengcai Liao and Ling Shao

Inception Institute of Artificial Intelligence (IIAI), Abu Dhabi, UAE

{scliao, ling.shao}@ieee.org

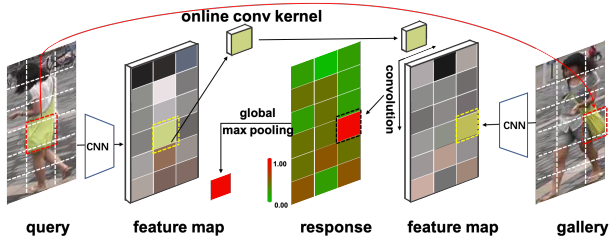


Figure 1. Illustration of the proposed QAConv method. We construct adaptive convolution kernels on the fly from query feature maps, and perform convolutions on gallery feature maps, followed by a global max pooling to find the best local correspondences.



Figure 2. Examples of the interpreted local correspondences from the output of the proposed QAConv image matching method.

Abstract

For person re-identification, existing deep networks often focus on representation learning. However, without domain adaptation or transfer learning, the learned model is fixed as is, which is not adaptable for handling various unseen scenarios. In this paper, beyond representation learning, we consider how to formulate person image matching directly in deep feature maps. We treat image matching as finding local correspondences in feature maps, and construct query-adaptive convolution kernels on the fly to achieve local matching. In this way, the matching process and result are interpretable, and this explicit matching is more generalizable than representation features to unseen scenarios, such as unknown misalignments, pose or viewpoint changes. To facilitate end-to-end training of this image matching architecture, we further build a class memory module to cache feature maps of the most recent samples of each class, so as to compute image matching losses for metric learning. Through direct cross-dataset evaluation without further transfer learning, the proposed Query-Adaptive Convolution (QAConv) method achieves better results than many transfer learning methods for person re-identification. Besides, a model-free temporal cooccurrence based score weighting method called TLift is proposed, which improves the performance to a further extent, resulting in state-of-the-art results in cross-dataset evaluations.

1. Introduction

Person re-identification is an active research topic in computer vision. It aims at finding the same person as the query image from a large volume of gallery images. With the progress in deep learning, person re-identification has been largely advanced in recent years. However, when generalization ability becomes an important concern, required by practical applications, existing methods usually lack satisfactory performance, evidenced by direct cross-dataset evaluation. To address this, many transfer learning, domain adaptation, and unsupervised learning methods, performed on the target domain, have been proposed. However, these methods require heavy computations in deployment, limiting their application in practical scenarios where the end-devices may have limited computation power.

Most existing person re-identification methods compute a fixed representation vector, also known as a feature vector, for each image, and employ a typical distance or similarity metric (e.g. Euclidean distance or cosine similarity) for image matching. Without domain adaptation or transfer learning, the learned model is fixed as is, which is not adaptable for handling various unseen scenarios. Therefore, when generalization ability is a concern, it is expected to have an adaptive ability for the given model architecture.

In this paper, we focus on generalizable and ready-to-use

person re-identification, through direct cross-dataset evaluation. Beyond representation learning, we consider how to formulate query-adaptive image matching directly in deep feature maps. Specifically, we treat image matching as finding local correspondences in feature maps, and construct query-adaptive convolution kernels on the fly to achieve local matching (see Fig. 1). In this way, the learned model benefits from adaptive convolution kernels in the final layer, specific to each image, and the matching process and result are interpretable (see Fig. 2), similar to traditional feature correspondence approaches [24, 3]. Probably because finding local correspondences through query-adaptive convolution is a common process among different domains, this explicit matching is more generalizable than representation features to unseen scenarios, such as unknown misalignments, pose or viewpoint changes. To facilitate end-to-end training of this Query-Adaptive Convolution (QAConv) architecture, we further build a class memory module to cache feature maps of the most recent samples of each class, so as to compute image matching losses for metric learning.

Through direct cross-dataset evaluation without further transfer learning, the proposed method achieves better results than many transfer learning methods for person re-identification. Besides, to explore the prior spatial-temporal structure of a camera network, a model-free temporal co-occurrence based score weighting method is proposed, named Temporal Lifting (TLift). This is also computed on the fly for each query image, without statistical learning of a transition time model in advance. As a result, TLift improves person re-identification to a further extent, resulting in state-of-the-art results in cross-dataset evaluation.

To summarize, the novelty of this work include (i) a new deep image matching approach with query-adaptive convolutions, along with a class memory module for end-to-end training, and (ii) a model-free temporal co-occurrence based score weighting method. The advantages of this work are also two-fold. First, the proposed image matching method is interpretable, it is well-suited in handling misalignments, pose or viewpoint changes, and it also generalizes well in unseen domains. Second, both QAConv and TLift can be computed on the fly, and they are complementary to many other methods. For example, QAConv does not require transfer learning, but can serve as a better pre-learned model for it, and TLift can be readily applied by most person re-identification algorithms as a post-processing step.

2. Related Works

Deep learning approaches have largely advanced person re-identification in recent years [34, 37, 62, 31, 55, 14, 33, 35, 57, 32, 17, 44, 52, 4]. However, due to limited labeled data and a big diversity in real-world surveillance, deep person re-identification methods usually have poor generalization ability in unseen scenarios. To address this, a number

of unsupervised transfer learning or domain adaption approaches have been proposed [28, 60, 7, 5, 48, 38, 15, 9, 16, 20, 61, 50, 47]. However, they require further training on the target domain, though mostly unsupervised or self-supervised. In practical applications, the end-devices may have limited computational power to support deep learning. Therefore, improving the baseline model’s generalization ability is still of urgent importance.

There are a number of person re-identification approaches proposed to deal with pose or viewpoint changes, and misalignments, for example, part-based feature representations [34, 37, 33], pose-adapted feature representations [53, 31], human parsing based representations [14], local neighborhood matching [1], and attentional networks [27, 45, 22, 29, 23, 43, 46, 35, 57, 32, 17, 44]. While these methods present high accuracy when trained and tested on the same dataset, their generalization ability to other datasets is mostly unknown.

For post-processing, re-ranking is a technique of refining matching scores, which further improves person re-identification accuracy [21, 51, 58, 31]. Besides, temporal information is also a useful cue to facilitate cross-camera person re-identification [25, 36]. While existing methods model transition times across different cameras but encounter difficulties in complex transition time distributions, the proposed TLift method applies co-occurrence constraint within each camera to avoid estimating transition times, and it is model-free and can be computed on the fly.

Recently, an exemplar memory is also proposed in ECN [61]. In contrast to the class memory module we use, exemplar memory caches feature vectors of every instance for unsupervised transfer learning, where KNN is applied for pseudo label assignment, and exemplar memory makes the instance-level KNN very convenient.

3. Query-adaptive Convolution

3.1. Query-adaptive Convolutional Matching

For face recognition and person re-identification, most existing methods do not explicitly consider the relationship between two input images under matching, but instead, like classification, they treat each image independently and apply the learned model to extract a fixed feature representation. Then, image matching is simply a distance measure between two representation vectors, regardless of the direct relationship between the actual contents of the two images.

In this paper, we consider the relationship between two images, and try to formulate adaptive image matching directly in deep feature maps. Specifically, we treat image matching as finding local correspondences in feature maps, and construct query-adaptive convolution kernels on the fly to achieve local matching. As shown in Fig. 1 and Fig. 3, to match two images, each image is firstly fed forward into

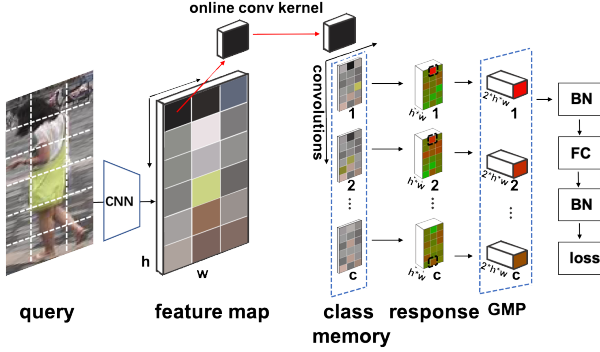


Figure 3. Architecture of the proposed QAConv.

a backbone CNN, resulting in a final feature map of size $[1, d, h, w]$, where d is the number of output channels, and h and w are the height and width of the feature map, respectively. Then, the channel dimension of both feature maps is normalized by the ℓ_2 -norm. After that, local patches of size $[s, s]$ at every location of the query feature map are extracted, and then reorganized into $[hw, d, s, s]$ as a convolution kernel, with input channels d , output channels hw , and kernel size $[s, s]$. This acts as a query-adaptive convolution kernel, with parameters constructed on the fly from the input, in contrast to fixed convolution kernels in the learned model. Upon this, the query-adaptive kernel can be used to perform a convolution on the normalized feature map of another image, resulting in $[1, hw, h, w]$ similarities.

Since feature channels are ℓ_2 -normalized, when $s = 1$, the convolution in fact measures the cosine similarity at every location of the two feature maps. Besides, since the convolution kernel is adaptively constructed from the image content, these similarity values exactly reflect the local matching results between the two input images. Therefore, an additional global max pooling (GMP) operation will output the best local matches, and the maximum indices found by GMP indicate the best locations of local correspondences, which can be further used to interpret the matching result, as illustrated in Fig. 2. Note that GMP can also be done by reshaping the $[1, hw, h, w]$ similarities and maximizing along the hw axis. That is, seeking the best matches can be carried out from both sides of the images. Concatenating the output will result in a $2hw$ similarity vector for each pair of images.

3.2. Network Architecture

The architecture of the proposed query-adaptive convolution based image matching method is shown in Fig. 3, which consists of a backbone CNN, the QAConv layer for local matching, a class memory layer for training (introduced below), a global max pooling layer, a BN-FC-BN block, and, finally, a similarity output by a sigmoid function for evaluation in the test phase or loss computation in the

training phase. The output size of the FC layer is 1, which acts as a binary classifier or a similarity metric, indicating whether or not one pair of images belongs to the same class. The two BN (batch normalization [12]) layers are all one-dimensional. They are used to normalize the similarity output and stabilize the gradient during training.

3.3. Class Memory and Update

To train the QAConv image matching architecture, we need to form sufficient training image pairs. A natural way to do this is to use mini batches for training, and form image pairs within each mini batch. However, this is not efficient for sampling the whole training set and the convergence is slow, since there are N^2 possible combinations of all sample pairs, where N is the number of training images. Therefore, we propose a class memory module to facilitate the end-to-end training of the QAConv network. Specifically, a $[c, d, h, w]$ tensor buffer is registered, where c is the number of classes. For each mini batch of size b , after the loss computation (introduced below), the $[b, d, h, w]$ feature map tensor of the mini batch will be updated into the memory buffer. We use a direct assignment update strategy, that is, each $[1, d, h, w]$ sample of class i from the mini batch will be assigned into location i of the $[c, d, h, w]$ memory buffer.

An exponential moving average update can also be used here. However, in our experience this is inferior to the direct replacement update. There might be two reasons for this. First, the replacement update caches feature maps of the most recent samples of each class, so as to reflect the most up-to-date state of the current model for loss computation. Second, since our task is to carry out image matching with local details in feature maps for correspondences, exponential moving average may smooth the local details of samples from the same class.

3.4. Loss Function

With a mini batch of size $[b, d, h, w]$ and class memory of size $[c, d, h, w]$, $b \times c$ pairs of similarity values will be computed by QAConv after the BN-FC-BN block. We use a sigmoid function to map the similarity values into $[0, 1]$, and compute the binary cross entropy loss. Considering that there are far more negative than positive pairs, to enable online hard negative mining while reducing the influence of the mass of negative pairs, we also apply the focal loss [19] to weight the binary cross entropy. That is,

$$\ell(\theta) = -\frac{1}{b} \sum_{i=1}^b \sum_{j=1}^c (1 - \hat{p}_{ij}(\theta))^\gamma \log(\hat{p}_{ij}(\theta)), \quad (1)$$

where θ is the network parameter, γ is the focusing parameter (by default $\gamma = 2$ as in [19]), and

$$\hat{p}_{ij} = \begin{cases} p_{ij} & \text{if } y_{ij} = 1, \\ 1 - p_{ij} & \text{otherwise,} \end{cases} \quad (2)$$



Figure 4. Illustration of the proposed TLift approach. A is the query person. E is more similar than A' to A in another camera. With nearby persons B and C , and their cross-camera top retrievals B' and C' acting as pivots, the score of A' near B' and C' can be temporally lifted, while the score of E will be reduced due to no such pivot.

where $y_{ij} = 1$ indicates a positive pair, while a negative pair otherwise, and $p_{ij} \in [0, 1]$ is the sigmoid probability.

4. Temporal Lifting

For person re-identification, to explore the prior spatial-temporal structure of a camera network, usually a transition time model is learned to measure the transition probability. However, for a complex camera network and various person transition patterns, it is not easy to learn a robust transition time distribution. In contrast, in this paper a model-free temporal cooccurrence based score weighting method is proposed, which is called Temporal Lifting (TLift). TLift does not model cross-camera transition times which could be variable and complex. Instead, TLift makes use of a group of nearby persons in each single camera, and find similarities between them. Fig. 4 illustrates the idea. A basic assumption is that people nearby in one camera are likely still nearby in another camera. Therefore, their corresponding matches in other cameras can serve as pivots to enhance the weights of other nearby persons. In Fig. 4, A is the query person. E is more similar than A' to A in another camera. With nearby persons B and C , and their top retrievals B' and C' acting as pivots, the matching score of A' can be temporally lifted since it is a nearby person of B' and C' , while the matching score of E will be reduced since there is no such pivot. Formally, suppose A is the query person in camera Q , then, the set of nearby persons to A in camera Q is defined as $R = \{B | \Delta T_{AB} < \tau, \forall B \in Q\}$, where ΔT_{AB} is the within-camera time difference between persons A and B , and τ is a threshold on ΔT to define nearby persons. Then, for each person in R , cross-camera person retrieval will be performed on a gallery camera G by QAConv, and the overall top K retrievals for R are defined as the pivot set P . Next, each person in the pivot set P acts

as an ensemble point for one-dimensional kernel density estimation on within-camera time differences on G , and the temporal matching probability between A and any person X in camera G will be computed as

$$p_t(A, X) = \frac{1}{|P|} \sum_{B \in P} e^{-\frac{\Delta T_{BX}^2}{\sigma^2}}, \quad (3)$$

where σ is the sensitivity parameter of the time difference. Then, this temporal probability is used to weight the QAConv similarity score using a multiplication fusion as $p(A, X) = (p_t(A, X) + \alpha)p_a(A, X)$, where $p_a(A, X)$ is the QAConv similarity, and α is a regularizer. This way, true positives near pivots will be lifted, while hard negatives far from pivots will be suppressed. Note that this is also computed on the fly for each query image, without learning a transition time model in advance. Therefore, it does not require training data, and can be readily applied by many other person re-identification methods.

5. Experiments

5.1. Implementation Details

The proposed method is implemented in PyTorch¹, based upon an adapted version [62] of the open source person re-identification library (open-reid)². Person images are resized to 384×128 . The backbone network is the Resnet152 [10], pre-trained on ImageNet. The layer3 feature map of the backbone network is used, since the size of the layer4 feature map is too small. A 1×1 convolution with 128 channels is further appended to reduce the final feature map size. The batch size of samples for training is 32. The SGD optimizer is applied, with a learning rate of 0.001 for the backbone network, and 0.01 for newly added layers. They are decayed by 0.1 after 40 epochs, and the training stops at 60 epochs. Considering the memory consumption and the efficiency, the kernel size of QAConv is set to $s = 1$. Parameters for TLift are $K = \tau = \sigma = 100$, and $\alpha = 0.1$.

A Random Block (RB) module is implemented for data augmentation of the QAConv training, similar to the Random Erasing (RE) method [59]. In the RE implementation, the target erasing area is sampled from a combination of random area and aspect ratio, which could exceed the original image height or width. Therefore, it needs to try multiple times (100 by default) to generate a reasonable region for erasing. In contrast, in our implementation of the RB module, a square block is used, with the size randomly sampled at most $0.8 \times width$ of the image. Then the square block is filled with white pixels. Note that with a simple square block, there is no need to sample multiple times of

¹Source code: <https://github.com/ShengcaiLiao/QAConv>

²<https://cysu.github.io/open-reid/>

areas and aspect ratios and check the validity, and hence the generation process is more efficient. Beyond this, only a random horizontal flipping is used for data augmentation.

5.2. Datasets

Experiments were conducted on three large person re-identification datasets, Market-1501 [54], DukeMTMC-reID [8, 56], and MSMT17 [39]. The Market-1501 dataset contains 32,668 images of 1501 identities captured from 6 cameras. There are 12,936 images from 751 identities for training, and 19,732 images from 750 identities for testing. The DukeMTMC-reID is a subset of the multi-target and multi-camera pedestrian tracking dataset DukeMTMC [8]. It includes 1,812 identities and 36,411 images, where 16,522 images of 702 identities are used for training, 2,228 images of another 702 identities are used as query images, and the remaining 17,661 images are used as gallery images. The MSMT17 dataset is the largest person re-identification dataset to date, which contains 4,101 identities and 126,441 images captured from 15 cameras. It is divided into a training set of 32,621 images from 1,041 identities, and a test set with the remaining images from 3,010 identities. Cross-dataset evaluation was performed in these datasets, by training on the training subset of one dataset (except that in MSMT17 we used all images for training following [50, 47]), and evaluating on the test subset of another dataset. The cumulative matching characteristic (CMC) and mean Average Precision (mAP) were used as the performance evaluation metrics. All evaluations followed the single-query evaluation protocol.

The Market-1501 and DukeMTMC-reID datasets are with frame numbers available, so that it is able to evaluate the proposed TLift method. The DukeMTMC-reID dataset has a good global and continuous record of frame numbers, and it is synchronized by providing offset times. In contrast, the Market-1501 dataset has only independent frame numbers for each session of videos from each camera. We simply made a cumulative frame record by assuming continuous video sessions. After that, frame numbers were converted to seconds in time by dividing the Frames Per Second (FPS) in video records, where FPS=59.94 for the DukeMTMC-reID dataset and FPS=25 for the Market-1501 dataset.

5.3. Ablation Study

Some ablation studies have been conducted to understand the proposed method, in the context of training on the Market-1501 training subset, while testing on the DukeMTMC-reID test subset. First, the role of the random block (RB) implementation as data augmentation is evaluated, compared to the random erasing (RE) method of [59]. From the results shown in Table 1, it can be observed that the new implementation of the RB module per-

Table 1. Role of random block, evaluated under Market→Duke.

Method	Rank-1 (%)	mAP (%)
QAConv without RE/RB	50.5	29.5
QAConv with RE [59]	51.6	30.6
QAConv with RB	54.4	33.6

forms better than the original RE implementation, as well as a baseline without RE or RB. This may be because the restricted square shape occludes person bodies within a local area. Besides, intuitively, RE/RB is useful for QAConv because random occlusion forces QAConv to learn various local correspondences, instead of only saliency but easy ones. Therefore, considering also the efficiency of the RB implementation, the new implementation is preferred in the training of the proposed QAConv algorithm.

Next, to understand the proposed QAConv loss, several other loss functions, including the classical softmax based cross entropy (CE) loss, the center loss [40, 13], the arc loss (derived from the ArcFace method [6] which is effective for face recognition), and the proposed class memory based loss, are evaluated for comparison. For these compared loss functions, the output of the final global average pooling layer of the Resnet network is used as feature representation, and the cosine similarity measure is adopted instead of the QAConv similarity. For the class memory loss, feature vectors are cached in memory instead of learnable parameters, and the same Eq. (1) is applied after calculating the cosine similarity values between mini-batch features and memory features. From the results shown in Table 2, it is obvious that the proposed QAConv method improves the existing loss functions by a large margin, with 13.7%-19.5% improvements at Rank-1, and 11.5%-15.2% improvements in mAP. Note that the class memory based loss only contributes small improvements over other baselines, indicating that the large improvement of QAConv is mainly due to the new matching mechanism, rather than the class memory based loss function. Besides, the arc loss published recently is one of the best face recognition method, but it does not seem to be so powerful when applied in person re-identification³. In our experience, the choice of loss functions does not largely influence person re-identification performance. Similar as in face recognition, existing studies [40, 6] show that new loss functions do have improvements, but cannot be regarded as significant ones over the softmax cross entropy baseline. Therefore, we may conclude that the large improvement observed here is due to the new matching scheme, instead of different loss configurations.

Furthermore, to understand the role of re-ranking (RR), the k-reciprocal encoding method [58] is applied upon QAConv. From results shown in Table 3, it can be seen that

³Parameters of arc loss were set according to [6]. We also tried several other values but did not get better results other than the defaults.

Table 2. Role of loss functions, evaluated under Market→Duke.

Method	Rank-1 (%)	mAP (%)
Softmax cross-entropy	34.9	18.4
Arc loss [6]	35.3	17.1
Center loss [40, 13]	38.9	22.1
Class memory loss	40.7	21.8
QAConv	54.4	33.6

Table 3. Performance (%) of different post-processing methods.

Method	Market→Duke		Duke→Market	
	Rank-1	mAP	Rank-1	mAP
QAConv	54.4	33.6	62.1	31.0
QAConv+RR [58]	61.8	52.4	68.2	51.2
QAConv+RR+TF [26]	70.7	61.9	68.8	46.9
QAConv+RR+TLift	66.7	56.0	74.4	56.6

enabling re-ranking do improve the performance a lot, especially with mAP, which is increased by 18.8% under Market→Duke, and 20.2% under Duke→Market. This improvement is much more significant based on QAConv than that based on other methods as reported in [58]. This is probably because the new QAConv matching scheme better measures the similarity between images, which benefits the reverse neighbor based re-ranking method. Note that the large improvement in mAP is important for the subsequent TLift, because it is relied on cross-camera top-k retrievals.

Next, based on QAConv and re-ranking, the contribution of TLift is evaluated, compared to a recent method called TFusion (TF) derived from [26]. From results shown in the last row of Table 3, it can be observed that employing TLift to explore temporal information further improves the results, with Rank-1 improved by 4.9%-6.2%, and mAP by 3.6%-5.4%. This improvement is complementary to re-ranking, so they can be combined. As for the existing method TFusion, it appears to be not stable, as a large improvement can be observed under Market→Duke, but little improvement can be obtain under Duke→Market, or even the mAP is clearly decreased⁴. This may be because TFusion is based on learning transition time distributions across cameras, which is not easy to handle complex camera networks and person transitions. In contrast, the proposed TLift method only depends on single-camera temporal information which is relatively more easy to handle.

Finally, to understand the effect of the backbone network, the QAConv results with the Resnet50 as backbone are also reported in Tables 4, 5, and 6. As can be observed, a larger network Resnet152 do have a better performance due to its larger learning capability. Meanwhile, it seems that this larger network, which contains more learnable parameters, does not have the overfitting problem when equipped with QAConv. Note that, though Resnet152 is a very large

⁴We have tried many different parameters for TFusion, but this is the best result that we can get.

network requiring heavy computation, in practice, it can be efficiently reduced by knowledge distillation [11].

5.4. Comparison to the State of the Arts

DukeMTMC-reID dataset. There are a great number of person re-identification methods since this is a very active research area. Here we only list recent results for comparison due to limited space. The cross-dataset evaluation results with the DukeMTMC-reID as the target dataset are listed in Table 4. Considering that many person re-identification methods employs the Resnet50 network, for a fair comparison, the QAConv results with the Resnet50 as backbone are also reported. Note that this paper mainly focuses on cross-dataset evaluation, especially direct evaluation without transfer learning. Therefore, some recent methods performing unsupervised learning on the target dataset are not compared here, such as the TAUDL [15], UTAL [16], and UGA [42], and also partially due to the fact that they use single-camera target labels for training. There are mainly three groups of methods listed in Table 4, namely GAN based methods, unsupervised transfer learning based methods, and direct cross-dataset evaluation based methods. The first two groups of methods require images from the target dataset for unsupervised learning, which are not directly comparable to the third one that directly evaluates on the target data to facilitate real applications. The proposed QAConv method belongs to the third group, together with some baselines of other recent methods.

As can be observed from Table 4, when trained on the Market-1501 dataset, the proposed QAConv method achieves the best performance in the direct evaluation group with a large margin, even with the Resnet50 backbone. When compared to GAN and transfer learning based methods, the QAConv method also outperforms most of them except three very recent methods, PAUL [47], ECN [61], and CDS [41], indicating that QAConv enables the network to learn how to match two person images, and the learned model generalizes well in unseen domains without transfer learning. Besides, by enabling re-ranking and TLift, the proposed method achieves the best result among all except Rank-1 of CDS. Note that the re-ranking and TLift methods can also be incorporated into other methods, though. Therefore, we list their results separately. However, both of these are calculated on the fly without learning in advance, so together with QAConv, it appears that a ready-to-use method with good generalization ability can also be achieved even without further domain adaptation, which is a nice solution considering that domain adaptation requires heavy computation for deep learning in deployment phase.

When taking MSMT17 as the source training data, the proposed QAConv method itself beats all other methods including transfer learning methods, clearly indicating its superiority in learning from large-scale data. This result is

Table 4. Comparison of the state-of-the-art cross-dataset evaluation results (%) with DukeMTMC-reID as the target dataset.

Method	Training		Test: Duke	
	Source	Target	R1	mAP
PTGAN, CVPR18 [39]	Market	Duke	27.4	-
SPGAN, CVPR18 [7]	Market	Duke	46.9	26.4
HHL, ECCV18 [60]	Market	Duke	46.9	27.2
CamStyle, TIP19 [62]	Market	Duke	51.7	27.7
PUL, TOMM18 [9]	Market	Duke	30.4	16.4
TJ-AIDL, CVPR18 [38]	Market	Duke	44.3	23.0
MMFA, BMVC18 [18]	Market	Duke	45.3	24.7
CFSM, AAI19 [5]	Market	Duke	49.8	27.3
PAUL, CVPR19 [47]	Market	Duke	56.1	35.7
ECN, CVPR19 [61]	Market	Duke	63.3	40.4
CDS, ICME19 [41]	Market	Duke	67.2	42.7
ECN, CVPR19 [61]	Market		28.9	14.8
PN-GAN, ECCV18 [30]	Market		29.9	15.8
QAConv (Resnet50)	Market		47.7	27.7
QAConv	Market		54.4	33.6
QAConv+RR	Market		61.8	52.4
QAConv+RR+TLift	Market		66.7	56.0
MAR, CVPR19 [50]	MSMT	Duke	67.1	48.0
PAUL, CVPR19 [47]	MSMT	Duke	72.0	53.2
MAR, CVPR19 [50]	MSMT		43.1	28.8
PAUL, CVPR19 [47]	MSMT		65.7	45.6
QAConv	MSMT		72.2	53.4
QAConv+RR	MSMT		78.1	72.4
QAConv+RR+TLift	MSMT		79.5	76.1

also the best one against all existing methods in Table 4 regardless of the training source. It is preferred in practice in the sense that, when trained with large-scale data, there may be no need to adapt the learned model in deployment.

Market-1501 dataset. Table 5 shows results with Market-1501 as the target dataset. Similarly, the QAConv method without transfer learning outperforms many transfer learning methods. Some transfer learning methods do achieve very good results, such as PAUL [47], CDS [41], and ECN [61]. However, they require heavy computational cost in deployment. When trained with MSMT17, the QAConv method itself also achieves the best performance against all existing methods except Rank-1 of ECN. This can be considered a large advancement in cross-dataset evaluation, which is a better evaluation strategy for understanding the generalization ability of algorithms.

MSMT17 dataset. Table 6 shows results with the MSMT17 dataset as the target dataset. Only the proposed QAConv requires no target data for training. However, it achieves almost the best performance with the same source training set, except that its mAP is slightly not as good as that of the ECN method. According to the comparison, it clearly indicates that the proposed QAConv method has a

Table 5. Comparison of the state-of-the-art cross-dataset evaluation results (%) with Market-1501 as the target dataset.

Method	Training		Test: Market	
	Source	Target	R1	mAP
PTGAN, CVPR18 [39]	Duke	Market	38.6	-
SPGAN, CVPR18 [7]	Duke	Market	58.1	26.9
CamStyle, TIP19 [62]	Duke	Market	64.7	30.4
HHL, ECCV18 [60]	Duke	Market	62.2	31.4
SyRI, ECCV18 [2]	Multi	Market	65.7	-
PUL, TOMM18 [9]	Duke	Market	44.7	20.1
TJ-AIDL, CVPR18 [38]	Duke	Market	58.2	26.5
MMFA, BMVC18 [18]	Duke	Market	56.7	27.4
CFSM, AAI19 [5]	Duke	Market	61.2	28.3
DECAMEL, TPAMI19 [49]	Multi	Market	60.2	32.4
PAUL, CVPR19 [47]	Duke	Market	66.7	36.8
CDS, ICME19 [41]	Duke	Market	71.6	39.9
ECN, CVPR19 [61]	Duke	Market	75.1	43.0
ECN, CVPR19 [61]	Duke		43.1	17.7
QAConv (Resnet50)	Duke		58.6	27.2
QAConv	Duke		62.1	31.0
QAConv+RR	Duke		68.2	51.2
QAConv+RR+TLift	Duke		74.4	56.6
MAR, CVPR19 [50]	MSMT	Market	67.7	40.0
PAUL, CVPR19 [47]	MSMT	Market	68.5	40.1
MAR, CVPR19 [50]	MSMT		46.2	24.6
PAUL, CVPR19 [47]	MSMT		59.3	31.0
QAConv	MSMT		73.9	46.6
QAConv+RR	MSMT		79.2	69.1
QAConv+RR+TLift	MSMT		85.7	75.1

Table 6. Comparison of the state-of-the-art cross-dataset evaluation results (%) with MSMT17 as the target dataset.

Method	Training		Test: MSMT	
	Source	Target	R1	mAP
DECAMEL, TPAMI19 [49]	Multi	MSMT	30.3	11.1
PTGAN [39], CVPR18	Market	MSMT	10.2	2.9
ECN, CVPR19 [61]	Market	MSMT	25.3	8.5
QAConv (Resnet50)	Market		21.5	6.3
QAConv	Market		25.6	8.2
QAConv+RR	Market		32.7	16.3
PTGAN [39], CVPR18	Duke	MSMT	11.8	3.3
ECN, CVPR19 [61]	Duke	MSMT	30.2	10.2
QAConv (Resnet50)	Duke		29.0	8.9
QAConv	Duke		31.8	10.0
QAConv+RR	Duke		40.4	20.2

relatively good generalization ability that without adaptation it is already comparable to other transfer learning approaches. Note that TLift cannot be applied for MSMT17.

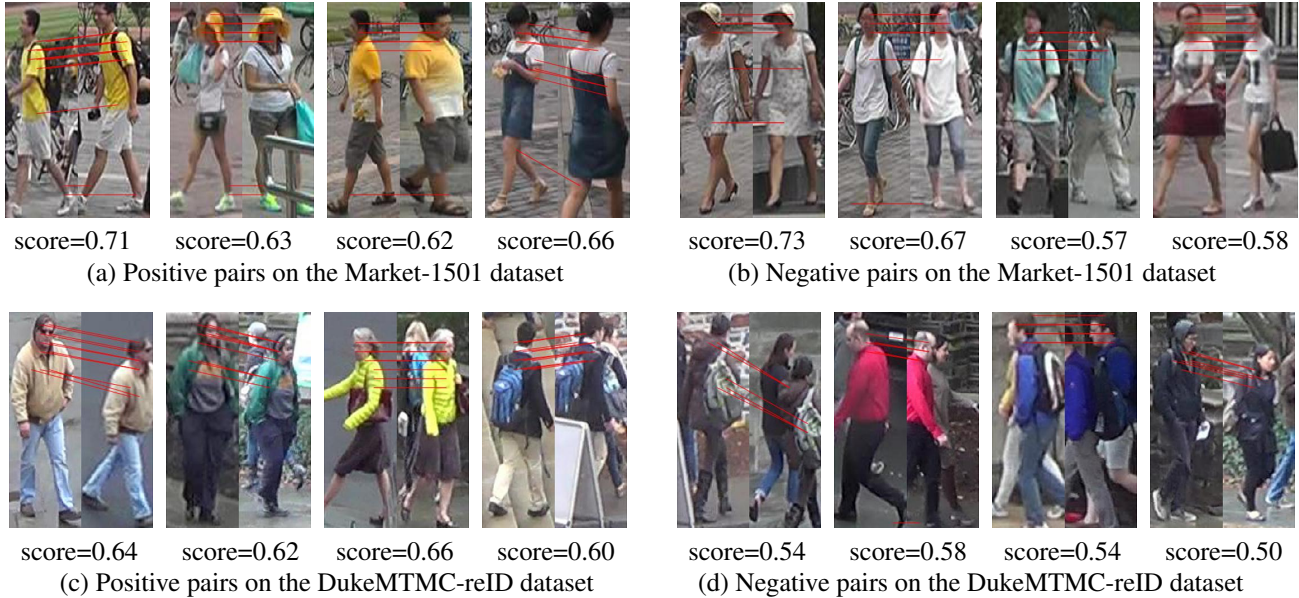


Figure 5. Examples of qualitative matching results by the proposed QAConv method using the model trained on the MSMT17 dataset.

5.5. Qualitative Analysis and Discussion

A unique characteristic of the proposed QAConv method is its interpretation ability of the matching. Therefore, we show some qualitative matching results in Fig. 5 for a better understanding of the proposed method. The model used here is trained on the MSMT17 dataset, and the evaluations are done on the query subsets of the Market-1501 and DukeMTMC-reID datasets. Results of both positive pairs and hard negative pairs are shown. Note that only reliable correspondences with matching scores over 0.5 are shown, and the local positions are coarse due to the 24×8 size of the feature map. As can be observed from Fig. 5, the proposed method is able to find correct local correspondences for positive pairs of images, even if there are notable misalignments in both scale and position, pose/viewpoint changes, occlusions, and mix up of other persons, thanks to the local matching mechanism of QAConv instead of global feature representations. Besides, for hard negative pairs, the matching of QAConv still appears to be mostly reasonable, by linking visually similar parts or even the same person (may be ambiguously labeled or walking closely to other persons). Note that the QAConv method gains the matching capability by automatic learning, from supervision of only class labels but not local correspondence labels. Besides, the matching capability seems to be also generalizable to other datasets beyond the training set.

The QAConv network is trained on an NVIDIA DGX-1 server, with two V100 GPU cards. With the backbone network Resnet152, the training time on the Market-1501 dataset is about 2.18 hours, and 2.85 hours on the DukeMTMC-reID dataset. The evaluation on the Market-

1501 dataset requires about 55 seconds for feature extraction, 38 seconds for QAConv similarity computation, 228 seconds for rerank, and 997 seconds for TLift. The evaluation on the DukeMTMC-reID dataset takes about 60 seconds for feature extraction, 25 seconds for QAConv similarity computation, 243 seconds for rerank, and 461 seconds for TLift. This is efficient, especially for RR+TLift, compared to transfer learning. Therefore, the overall solution of QAConv+RR+TLift is preferred in practical applications.

One drawback of QAConv is that it requires more memory to run than other methods, and it needs to store feature maps of images, rather than features, where feature maps are generally larger in size than representation features. Besides, TLift can only be applied on datasets with good time records. Though this information is easy to obtain in real surveillance, most existing person re-identification datasets do not contain it. Another drawback of TLift is that it cannot be applied to arbitrary query images beyond a camera network, though once an initial match is found, it can be used to refine the search.

6. Conclusion

In this paper, beyond representation learning, we formulate image matching directly in deep feature maps and develop a deep image matching method called QAConv for person re-identification. It is able to find local correspondences in feature maps by constructing query-adaptive convolution kernels on the fly for local matching. A good property of QAConv is that its matching result is interpretable, and this explicit matching is more generalizable than representation features to unseen scenarios. A model-free tempo-

ral cooccurrence based score weighting method called TLift is also proposed, which achieves further improvement with temporal information. The proposed method achieves state-of-the-art results in cross-dataset person re-identification. In future research, it would be interesting to apply QACnv to other image matching scenarios, such as face recognition.

References

- [1] Ejaz Ahmed, Michael Jones, and Tim K Marks. An improved deep learning architecture for person re-identification. In *Proceedings of the IEEE Conference on Computer Vision and Pattern Recognition*, pages 3908–3916, 2015. 2
- [2] Slawomir Bak, Peter Carr, and Jean-Francois Lalonde. Domain adaptation through synthesis for unsupervised person re-identification. In *Proceedings of the European Conference on Computer Vision (ECCV)*, pages 189–205, 2018. 7
- [3] Herbert Bay, Tinne Tuytelaars, and Luc Van Gool. Speeded-up robust features (SURF). *Computer Vision and Image Understanding*, 110(3):346–359, 2008. 2
- [4] Xiaobin Chang, Timothy M Hospedales, and Tao Xiang. Multi-level factorisation net for person re-identification. In *Proceedings of the IEEE Conference on Computer Vision and Pattern Recognition*, pages 2109–2118, 2018. 2
- [5] Xiaobin Chang, Yongxin Yang, Tao Xiang, and Timothy M Hospedales. Disjoint label space transfer learning with common factorised space. *arXiv preprint arXiv:1812.02605*, 2018. 2, 7
- [6] Jiankang Deng, Jia Guo, Niannan Xue, and Stefanos Zafeiriou. Arcface: Additive angular margin loss for deep face recognition. In *Proceedings of the IEEE Conference on Computer Vision and Pattern Recognition*, pages 4690–4699, 2019. 5, 6
- [7] Weijian Deng, Liang Zheng, Qixiang Ye, Guoliang Kang, Yi Yang, and Jianbin Jiao. Image-image domain adaptation with preserved self-similarity and domain-dissimilarity for person reidentification. In *Proceedings of IEEE Computer Society Conference on Computer Vision and Pattern Recognition*, 2018. 2, 7
- [8] R. Ergys, S. Francesco, Z. Roger, C. Rita, and T. Carlo. Performance measures and a data set for multi-target, multi-camera tracking. In *ECCV workshop on Benchmarking Multi-Target Tracking*, 2016. 5
- [9] H. Fan, L. Zheng, C. Yan, and Y. Yang. Unsupervised person re-identification: Clustering and fine-tuning. *TOMM*, 14(4):83, 2018. 2, 7
- [10] K. He, X. zhang, S. Ren, and J. Sun. Deep residual learning for image recognition. In *Proceedings of IEEE Computer Society Conference on Computer Vision and Pattern Recognition*, pages 770–778, 2016. 4
- [11] Geoffrey Hinton, Oriol Vinyals, and Jeff Dean. Distilling the knowledge in a neural network. *arXiv preprint arXiv:1503.02531*, 2015. 6
- [12] Sergey Ioffe and Christian Szegedy. Batch normalization: Accelerating deep network training by reducing internal covariate shift. *arXiv preprint arXiv:1502.03167*, 2015. 3
- [13] Haibo Jin, Xiaobo Wang, Shengcai Liao, and Stan Z Li. Deep person re-identification with improved embedding and efficient training. In *2017 IEEE International Joint Conference on Biometrics (IJCB)*, pages 261–267. IEEE, 2017. 5, 6
- [14] Mahdi M Kalayeh, B. Emrah, Muhittin Gökmen, Mustafa E Kamasak, and Mubarak Shah. Human semantic parsing for person re-identification. In *Proceedings of IEEE Computer Society Conference on Computer Vision and Pattern Recognition*, pages 1062–1071, 2018. 2
- [15] M. Li, X. Zhu, and S. Gong. Unsupervised person re-identification by deep learning tracklet association. *arXiv preprint arXiv:1809.02874*, 2018. 2, 6
- [16] Minxian Li, Xiatian Zhu, and Shaogang Gong. Unsupervised tracklet person re-identification. *TPAMI*, 2019. 2, 6
- [17] Wei Li, Xiatian Zhu, and Shaogang Gong. Harmonious attention network for person re-identification. In *Proceedings of the IEEE Conference on Computer Vision and Pattern Recognition*, pages 2285–2294, 2018. 2
- [18] S. Lin, H. Li, Chang-Tsun Li, and Alex Chichung Kot. Multi-task mid-level feature alignment network for unsupervised cross-dataset person re-identification. *arXiv preprint arXiv:1807.01440*, 2018. 7
- [19] Tsung-Yi Lin, Priya Goyal, Ross Girshick, Kaiming He, and Piotr Dollár. Focal loss for dense object detection. In *Proceedings of the IEEE international conference on computer vision*, pages 2980–2988, 2017. 3
- [20] Yutian Lin, Xuanyi Dong, Liang Zheng, Yan Yan, and Yi Yang. A bottom-up clustering approach to unsupervised person re-identification. In *AAAI Conference on Artificial Intelligence*, volume 2, 2019. 2
- [21] Chunxiao Liu, Chen Change Loy, Shaogang Gong, and Guijin Wang. Pop: Person re-identification post-rank optimisation. In *International Conference on Computer Vision*, 2013. 2
- [22] Hao Liu, Jiashi Feng, Meibin Qi, Jianguo Jiang, and Shuicheng Yan. End-to-end comparative attention networks for person re-identification. *IEEE Transactions on Image Processing*, 26(7):3492–3506, 2017. 2
- [23] Xihui Liu, Haiyu Zhao, Maoqing Tian, Lu Sheng, Jing Shao, Shuai Yi, Junjie Yan, and Xiaogang Wang. Hydraplus-net: Attentive deep features for pedestrian analysis. In *Proceedings of the IEEE international conference on computer vision*, pages 350–359, 2017. 2
- [24] David G Lowe. Distinctive image features from scale-invariant keypoints. *International journal of computer vision*, 60(2):91–110, 2004. 2
- [25] J. Lv, W. Chen, Q. Li, and C. Yang. Unsupervised cross-dataset person re-identification by transfer learning of spatial-temporal patterns. In *Proceedings of IEEE Computer Society Conference on Computer Vision and Pattern Recognition*, pages 7948–7956, 2018. 2
- [26] Jianming Lv, Weihang Chen, Qing Li, and Can Yang. Unsupervised cross-dataset person re-identification by transfer learning of spatial-temporal patterns. In *2018 IEEE Conference on Computer Vision and Pattern Recognition, CVPR 2018, Salt Lake City, UT, USA, June 18-22, 2018*, pages 7948–7956, 2018. 6

- [27] Volodymyr Mnih, Nicolas Heess, Alex Graves, et al. Recurrent models of visual attention. In *Advances in neural information processing systems*, pages 2204–2212, 2014. 2
- [28] P. Peng, T. Xiang, Y. Wang, P. Massimiliano, S. Gong, T. Huang, and Y. Tian. Unsupervised cross-dataset transfer learning for person re-identification. In *Proceedings of IEEE Computer Society Conference on Computer Vision and Pattern Recognition*, pages 1306–1315, 2016. 2
- [29] Xuelin Qian, Yanwei Fu, Yu-Gang Jiang, Tao Xiang, and Xiangyang Xue. Multi-scale deep learning architectures for person re-identification. In *Proceedings of the IEEE International Conference on Computer Vision*, pages 5399–5408, 2017. 2
- [30] Xuelin Qian, Yanwei Fu, Tao Xiang, Wenxuan Wang, Jie Qiu, Yang Wu, Yu-Gang Jiang, and Xiangyang Xue. Pose-normalized image generation for person re-identification. In *Proceedings of the European Conference on Computer Vision (ECCV)*, pages 650–667, 2018. 7
- [31] M Saquib Sarfraz, Arne Schumann, Andreas Eberle, and Rainer Stiefelhagen. A pose-sensitive embedding for person re-identification with expanded cross neighborhood re-ranking. In *Proceedings of the IEEE Conference on Computer Vision and Pattern Recognition*, pages 420–429, 2018. 2
- [32] Jianlou Si, Honggang Zhang, Chun-Guang Li, Jason Kuen, Xiangfei Kong, Alex C Kot, and Gang Wang. Dual attention matching network for context-aware feature sequence based person re-identification. In *Proceedings of the IEEE Conference on Computer Vision and Pattern Recognition*, pages 5363–5372, 2018. 2
- [33] Yumin Suh, Jingdong Wang, Siyu Tang, Tao Mei, and Kyoung Mu Lee. Part-aligned bilinear representations for person re-identification. In *Proceedings of the European Conference on Computer Vision (ECCV)*, pages 402–419, 2018. 2
- [34] Yifan Sun, Liang Zheng, Yi Yang, Qi Tian, and Shengjin Wang. Beyond part models: Person retrieval with refined part pooling (and a strong convolutional baseline). In *Proceedings of the European Conference on Computer Vision (ECCV)*, 2018. 2
- [35] Cheng Wang, Qian Zhang, Chang Huang, Wenyu Liu, and Xinggang Wang. Mancs: A multi-task attentional network with curriculum sampling for person re-identification. In *Proceedings of the European Conference on Computer Vision (ECCV)*, pages 365–381, 2018. 2
- [36] Guangcong Wang, Jianhuang Lai, Peigen Huang, and Xiaohua Xie. Spatial-temporal person re-identification. In *AAAI Conference on Artificial Intelligence*, 2019. 2
- [37] Guanshuo Wang, Yufeng Yuan, Xiong Chen, Jiwei Li, and Xi Zhou. Learning discriminative features with multiple granularities for person re-identification. In *2018 ACM Multimedia Conference on Multimedia Conference*, pages 274–282. ACM, 2018. 2
- [38] J. Wang, X. Zhu, S. Gong, and W. Li. Transferable joint attribute-identity deep learning for unsupervised person re-identification. *arXiv preprint arXiv:1803.09786*, 2018. 2, 7
- [39] Longhui Wei, Shiliang Zhang, Wen Gao, and Qi Tian. Person transfer gan to bridge domain gap for person re-identification. In *Proceedings of the IEEE Conference on Computer Vision and Pattern Recognition*, pages 79–88, 2018. 5, 7
- [40] Yandong Wen, Kaipeng Zhang, Zhifeng Li, and Yu Qiao. A discriminative feature learning approach for deep face recognition. In *European conference on computer vision*, pages 499–515. Springer, 2016. 5, 6
- [41] Jinlin Wu, Shengcai Liao, Xiaobo Wang, Yang Yang, Stan Z Li, et al. Clustering and dynamic sampling based unsupervised domain adaptation for person re-identification. In *2019 IEEE International Conference on Multimedia and Expo (ICME)*, pages 886–891. IEEE, 2019. 6, 7
- [42] Jinlin Wu, Yang Yang, Hao Liu, Shengcai Liao, Zhen Lei, and Stan Z Li. Unsupervised graph association for person re-identification. In *Proceedings of the IEEE International Conference on Computer Vision*, pages 8321–8330, 2019. 6
- [43] Lin Wu, Yang Wang, Xue Li, and Junbin Gao. What-and-where to match: deep spatially multiplicative integration networks for person re-identification. *Pattern Recognition*, 76:727–738, 2018. 2
- [44] Jing Xu, Rui Zhao, Feng Zhu, Huaming Wang, and Wanli Ouyang. Attention-aware compositional network for person re-identification. In *Proceedings of the IEEE Conference on Computer Vision and Pattern Recognition*, pages 2119–2128, 2018. 2
- [45] Kelvin Xu, Jimmy Ba, Ryan Kiros, Kyunghyun Cho, Aaron Courville, Ruslan Salakhudinov, Rich Zemel, and Yoshua Bengio. Show, attend and tell: Neural image caption generation with visual attention. In *International conference on machine learning*, pages 2048–2057, 2015. 2
- [46] Shuangjie Xu, Yu Cheng, Kang Gu, Yang Yang, Shiyu Chang, and Pan Zhou. Jointly attentive spatial-temporal pooling networks for video-based person re-identification. In *Proceedings of the IEEE International Conference on Computer Vision*, pages 4733–4742, 2017. 2
- [47] Qize Yang, Hong-Xing Yu, Ancong Wu, and Wei-Shi Zheng. Patch-based discriminative feature learning for unsupervised person re-identification. In *Proceedings of the IEEE Conference on Computer Vision and Pattern Recognition*, pages 3633–3642, 2019. 2, 5, 6, 7
- [48] H. Yu, A. Wu, and W. Zheng. Cross-view asymmetric metric learning for unsupervised person re-identification. In *Proceedings of IEEE International Conference on Computer Vision*, 2017. 2
- [49] Hong-Xing Yu, Ancong Wu, and Wei-Shi Zheng. Unsupervised person re-identification by deep asymmetric metric embedding. *IEEE transactions on pattern analysis and machine intelligence*, 2019. 7
- [50] Hong-Xing Yu, Wei-Shi Zheng, Ancong Wu, Xiaowei Guo, Shaogang Gong, and Jian-Huang Lai. Unsupervised person re-identification by soft multilabel learning. In *Proceedings of the IEEE Conference on Computer Vision and Pattern Recognition*, pages 2148–2157, 2019. 2, 5, 7
- [51] Rui Yu, Zhichao Zhou, Song Bai, and Xiang Bai. Divide and fuse: A re-ranking approach for person re-identification. *arXiv preprint arXiv:1708.04169*, 2017. 2

- [52] Ying Zhang, Tao Xiang, Timothy M Hospedales, and Huchuan Lu. Deep mutual learning. In *Proceedings of the IEEE Conference on Computer Vision and Pattern Recognition*, pages 4320–4328, 2018. 2
- [53] Haiyu Zhao, Maoqing Tian, Shuyang Sun, Jing Shao, Junjie Yan, Shuai Yi, Xiaogang Wang, and Xiaoou Tang. Spindle net: Person re-identification with human body region guided feature decomposition and fusion. In *Proceedings of the IEEE Conference on Computer Vision and Pattern Recognition*, pages 1077–1085, 2017. 2
- [54] L. Zheng, L. Shen, L. Tian, S. Wang, J. Wang, and Q. Tian. Scalable person re-identification: A benchmark. In *Proceedings of IEEE International Conference on Computer Vision*, 2015. 5
- [55] Zhedong Zheng, Xiaodong Yang, Zhiding Yu, Liang Zheng, Yi Yang, and Jan Kautz. Joint Discriminative and Generative Learning for Person Re-identification. In *Proceedings of the IEEE Conference on Computer Vision and Pattern Recognition*, 2019. 2
- [56] Zhedong Zheng, Liang Zheng, and Yi Yang. Unlabeled samples generated by gan improve the person re-identification baseline in vitro. *international conference on computer vision*, pages 3774–3782, 2017. 5
- [57] Zhedong Zheng, Liang Zheng, and Yi Yang. Pedestrian alignment network for large-scale person re-identification. *IEEE Transactions on Circuits and Systems for Video Technology*, 2018. 2
- [58] Zhun Zhong, Liang Zheng, Donglin Cao, and Shaozi Li. Re-ranking person re-identification with k-reciprocal encoding. In *Proceedings of the IEEE Conference on Computer Vision and Pattern Recognition*, pages 1318–1327, 2017. 2, 5, 6
- [59] Zhun Zhong, Liang Zheng, Guoliang Kang, Shaozi Li, and Yi Yang. Random erasing data augmentation. *arXiv preprint arXiv:1708.04896*, 2017. 4, 5
- [60] Z. Zhong, L. Zheng, S. Li, and Y. Yang. Generalizing a person retrieval model hetero-and homogeneously. In *Proceedings of the European Conference on Computer Vision (ECCV)*, pages 172–188, 2018. 2, 7
- [61] Zhun Zhong, Liang Zheng, Zhiming Luo, Shaozi Li, and Yi Yang. Invariance matters: Exemplar memory for domain adaptive person re-identification. In *Proceedings of the IEEE Conference on Computer Vision and Pattern Recognition*, pages 598–607, 2019. 2, 6, 7
- [62] Z. Zhong, L. Zheng, Z. Zheng, S. Li, and Y. Yang. Camstyle: A novel data augmentation method for person re-identification. *IEEE Transactions on Image Processing*, 2018. 2, 4, 7